AIP | Journal of Applied Physics

Open photoacoustic cell for thermal diffusivity measurements of a fast hardening cement used in dental restoring

F. B. G. Astrath, N. G. C. Astrath, M. L. Baesso, A. C. Bento, J. C. S. Moraes et al.

Citation: J. Appl. Phys. **111**, 014701 (2012); doi: 10.1063/1.3673873
View online: http://dx.doi.org/10.1063/1.3673873
View Table of Contents: http://jap.aip.org/resource/1/JAPIAU/v111/i1
Published by the AIP Publishing LLC.

Open photoacoustic cell for thermal diffusivity measurements of a fast hardening cement used in dental restoring

F. B. G. Astrath,[1] N. G. C. Astrath,[1,a)] M. L. Baesso,[1] A. C. Bento,[1] J. C. S. Moraes,[2] and A. D. Santos[2]
[1]*Universidade Estadual de Maringá, Grupo de Estudo dos Fenômenos Fotoacústicos e Fototérmicos, Departamento de Física, Av. Colombo 5790, Maringá - PR 87020-900, Brazil*
[2]*UNESP – University Estadual Paulista, Campus de Ilha Solteira, Departamento de Física e Química, Av. Brasil 56, Ilha Solteira - SP 15385-000, Brazil*

(Received 2 August 2011; accepted 7 December 2011; published online 5 January 2012)

Thermal diffusivity and conductivity of dental cements have been studied using open photoacoustic cell (OPC). The samples consisted of fast hardening cement named CER, developed to be a root-end filling material. Thermal characterization was performed in samples with different gel/powder ratio and particle sizes and the results were compared to the ones from commercial cements. Complementary measurements of specific heat and mass density were also performed. The results showed that the thermal diffusivity of CER tends to increase smoothly with gel volume and rapidly against particle size. This behavior was linked to the pores size and their distribution in the samples. The OPC method was shown to be a valuable way in deriving thermal properties of porous material. © *2012 American Institute of Physics*. [doi:10.1063/1.3673873]

I. INTRODUCTION

Photothermal (PT) techniques have been shown to be highly sensitive tools and have been applied to determine thermo-optical properties of materials.[1–3] PT techniques are based on the photoinduced heat generation by nonradiative decay process following optical energy absorption of a sample and the heat can cause a number of different effects, which provide various detection mechanisms. The information of the temperature rise in the sample as well as its thermo-physical parameters can be obtained with these detection methods.[4,5] In particular, photoacoustic (PA) spectroscopy is an important technique because it allows studies in nonhomogeneous materials; it is nondestructive and demands minimal sample preparation.[6–10] Since the PA signal responds only to the absorbed light, the effects of scattered light play no significant roles in the measurements. Apart from several different apparatuses for the PA detection, the simplicity and the usefulness of the open-photoacoustic-cell (OPC) make this technique easily applicable to thermal characterization of solid materials such as the measurement of thermal diffusivity and thermal conductivity.[11–14]

Mineral Trioxide Aggregate (MTA) is the most popular material used in dentistry. MTA is composed of a white or gray powder of fine hydrophilic particles consisting of compounds of tricalcium silicate, tricalcium oxide, tricalcium aluminate, and silicate oxide.[15] It was first described by Lee and co-authors[15] and reviewed by Parirokh and Torabinejad.[16] Since the first report, it has been widely investigated and proved to be an excellent dental material due to its good physical, chemical, and biologic properties. Indeed, the importance of studying advanced materials accompanying the updated technology is of fundamental importance. The knowledge of thermal properties of a dental material helps defining the biocompatibility between restored and natural teeth.

Recently, a fast setting cement named CER has been developed. It is biocompatible cement used as a root-end filling material,[17] and is presented as a gray or white powder made to mix with a gelatinous emulsificant that gives to the mixture a better consistence improving the setting time comparing with other similar cements. The CER cement has a short setting time and better handling when compared to others MTA materials (e.g., Angelus and Pro-Root Dentsply), improving the clinical procedure when used as root-end filling material.[18] Therefore, CER is a promising biocompatible material for which the measurements of the thermophysical properties may help to understand its behavior when used in pre-clinical tests.

This work presents the thermal characterization of a set of gray CER samples using the OPC technique and compares their thermal properties to those of human teeth and other brands already used by professionals in dental field. Additional measurements of the specific heat (c), mass density (ρ), and porosity of the samples were performed, allowing to obtain the thermal conductivity (k). The results were compared with the thermal properties of commercial cements. The physical properties dependence on the preparing conditions upon emulsion volume and grain particle size were investigated. It is shown that thermal diffusion is extremely sensitive to the grain size and porosity of the cement.

II. THEORY

In the OPC experiment performed in this work, a plate-shaped solid samples surrounded by air with the edges tightly fixed in the photoacoustic cell is heated by an excitation laser beam of radius ω. In this condition, the mechanisms generating the pressure variation inside the PA chamber are the thermal diffusion and the thermoelastic

a)Author to whom correspondence should be addressed. Electronic mail: astrathngc@pq.cnpq.br.

bending. The thermoelastic bending is essentially due to the temperature gradient inside the sample along the thickness axis (z axis), which leads the thermal expansion to depend on z. This z-dependence of the displacement along the radial direction induces a bending of the sample in the z direction that acts as a mechanical piston, thereby contributing to the PA signal. The contribution from the sample bending to the PA signal is calculated by solving the thermoelastic equations, whereas the thermal diffusion contribution is attained by solving the heat conduction differential equation, as described in details in Refs. 12, 18–20. Assuming that all light is absorbed at the sample surface and considering no axial heat flux, the pressure fluctuation in the air chamber of a photoacoustic cell due to thermal diffusion (TD) and thermoelastic (TE) bending of a thermally thick sample, i.e., $l_s a_s \gg 1$, is expressed in one-dimension by[12,18–20]

$$P = e^{j(\omega t-\pi/2)}\left\{\frac{C_1}{\sigma_s\sigma_g}\frac{1}{\sinh(l_s\sigma_s)}+ \right. \\ \left. +\frac{C_1C_2}{\sigma_s^2\sigma_g}\left(\frac{\cosh(\sigma_s l_s)-(\sigma_s l_s/2)\sinh(\sigma_s l_s)-1}{\sinh(\sigma_s l_s)}\right)\right\}, \quad (1)$$

in which $C_1 = \gamma P_0\beta I_0/\left(T_0 k_s l_g\right)$ and $C_2 = 3R'^4 T_0\alpha_T\sqrt{\alpha_s/\alpha_g}/\left(R^2 l_s^3\right)$. Here, R' is the radius of the sample and R is the radius of the PA chamber in front of the microphone. α_T is the sample thermal expansion coefficient. γ is the specific heat ratio of the gas in the chamber; P_0 and T_0 are the ambient pressure and temperature, respectively. I_0 is the absorbed light intensity; $\omega = 2\pi f$ and f is the modulation frequency. l_i, k_i, and α_i are the thickness, thermal conductivity, and thermal diffusivity of material i, respectively. Here the subscript i denotes the sample (s) and the gas (g) medium. $\sigma_i = (1+j)a_i$, and $a_i = (\pi f/\alpha_i)^{1/2}$ is the thermal diffusion coefficient of material i. The first term in Eq. (1) is due to the heat diffusion contribution to the pressure fluctuation whereas the second represents the thermoelastic one.

Equation (1) presents very distinct frequency regimes and depends strongly on the thermal diffusivity and on the thermoelastic strength parameter (C_2). Figures 1(a) and 1(b) show the dependences of Eq. (1) on frequency, thermal diffusivity, and C_2. The thermal diffusivity of the gas, air in this case, is 0.2 cm^2/s and the sample thickness $l_s = 100$ μm. One can observe a minimum in the plot of $\ln(|P.P^*|)^{1/2}$ against $\ln(f)$ that is dependent on the thermal diffusivity, Fig. 1(a). This minimum shifts to higher frequencies as the thermal diffusivity increases. The influence of the coefficient C_2 is presented in Fig. 1(b), which also shows a minimum that is smoothed as C_2 increases.

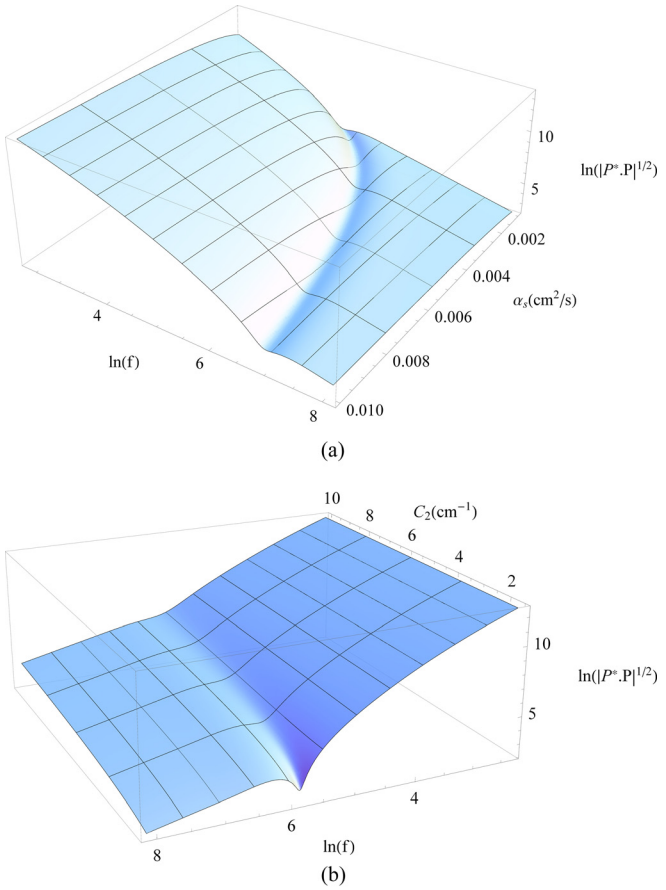

FIG. 1. (Color online) (a) Dependence of $\ln(|P.P^*|)^{1/2}$ vs $\ln(f)$ on the thermal diffusivity and (b) on the parameter C_2. The air thermal diffusivity is $\alpha_g = 0.2$ cm^2/s and the sample thickness $l_s = 100$ μm.

III. EXPERIMENTAL SETUP

The experimental OPC system for performing the frequency scans of the samples is shown in Fig. 2. It consisted of a 100 mW diode laser at 532 nm (B&W Tek inc.) mechanically chopped from 4 to 300 Hz (SR540, Stanford Research System) and uniformly focused directly onto the sample with a spot size of 2 mm. The sample was attained using a small amount of vacuum grease on top of a electret microphone as shown in Fig. 2 with a hollow of 2 mm in diameter (R = 1 mm). A lockin amplifier (SR830, Stanford Research System) is used to analyze the amplitude of the microphone signal. This electret microphone has a non-flat frequency response from 4 to 300 Hz. Its frequency response was obtained by running a frequency scan of a 60 μm-thick aluminum sample. This sample is thermally thin ($l_s a_s \ll 1$) up to 10 kHz, and one would expect the dependence of the PA signal on the modulation frequency to be $f^{-1.5}$.[12]

Complementary measurements of specific heat and mass density, both at room temperature, were performed using a homemade thermal relaxation calorimeter[21] and a standard Archimedes method, respectively. A laser beam was used as the heat source for the calorimeter, as described in Ref. 21. The samples used in these measurements were 1 mm thick with about 30 mg, condition which the internal relaxation time is negligible.[21] The porosity measurements were performed by the mercury intrusion technique on high pressure.

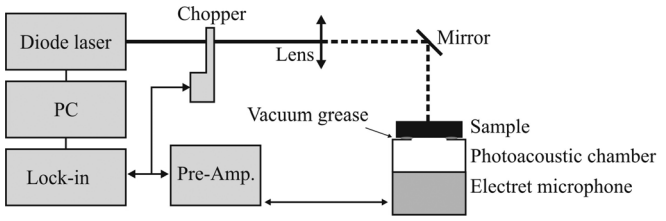

FIG. 2. OPC experimental setup.

IV. SAMPLE PREPARATION

Three types of materials were investigated in this work: two commercial cements and the CER samples. The commercial cements are MTA-Angelus[22] (Angelus Indústria de Materiais Odontológicos) and Portland cement (Cia Cimento Itambé). The CER samples formula are based on Portland cement clinker, barium sulfate (radiopacifier), and a gel composed of water and an emulsifier with the function of improving the handling properties of the paste. Both commercial samples were tested to compare the results with the CER samples. All samples are optically opaque.

For the measurement of the thermal diffusivity, powder of MTA-Angelus and Portland cements were mixed with distilled water on a glass plate with a steel spatula in the proportion recommended by their manufactures and the final samples were disks of radius $R' = 5\,\text{mm}$ and thickness between 300–500 μm. For CER, the procedure was the same, but varying the gel volume from 140 to 170 μL in steps of 10 μL and fixing 650 mg for each batch. Before preparation, the CER powders were selected with different granulations using the following sieves size: <25, <38, <45, and <53 μm.

V. RESULTS AND DISCUSSION

Figure 3 shows a typical normalized OPC signal for the CER sample ($l_s = 350\mu$m) with granulation <25 μm and gel volume of 160 μL (CER25-160 μL). The frequency dependence of the OPC signal clearly confirms the TD and TE contributions, which presents similar trend as the ones displayed in Figs. 1(a) and 1(b). The solid line in Fig. 3 corresponds to the least-square fit of the data to the theoretical expression obtained from Eq. (1). For comparison, the dotted line shows the TD contribution separately (using $C_2 = 0$). The fitting was performed considering fixed the gas (air in this case) thermal diffusivity, $\alpha_g = 0.2\ \text{cm}^2/\text{s}$.

Figure 4 shows the thermal diffusivities of all samples with different grain sizes as a function of gel volume. A set of at least two samples of each granulation and gel volume were measured three times to obtain the error bars. The results are also presented in Table I, which also includes values of the thermal diffusivity of MTA - Angelus, Portland

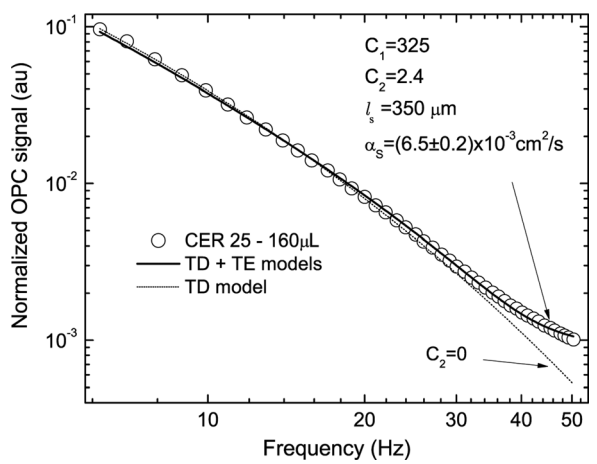

FIG. 3. Normalized OPC amplitude as a function of the modulation frequency for the CER sample with granulation <25 μm and gel volume of 160 μL (CER25-160 μL). Solid line represents the data fit to Eq. (1).

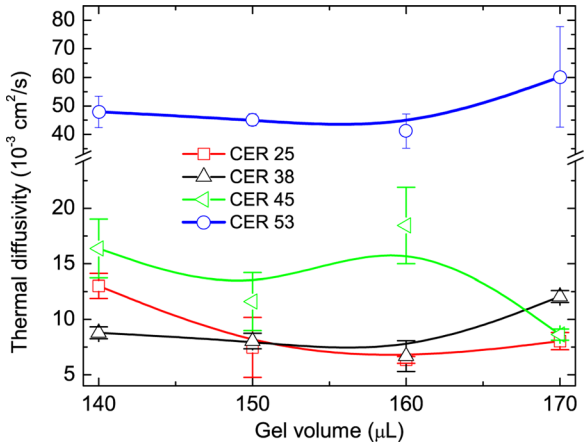

FIG. 4. (Color online) OPC results for thermal diffusivity of CER as a function of gel volume.

cement and other literature values for materials used in dental restoration.[23] The values found in the literature for the teeth and enamel are: $\alpha_s = 7.4 \times 10^{-3}\text{cm}^2/\text{s}$[24] and $\alpha_s = 4.2 \times 10^{-3}\text{cm}^2/\text{s}$,[25] respectively.

The thermal diffusivity values as a function of gel volume present similar behavior for different granulation sizes, apart from CER 45. A decreasing in the thermal diffusivity is observed as the gel volume increased from 140 to 160 μL. A minimum can be observed in the values of α_s around 160 μL of gel. With regard to particle size, the thermal diffusivity increased for all gel-to-powder proportions when the range of particle size was increased.

Information on the thermal expansion can also be obtained by the fit parameters C_2 and α_s with $\alpha_T = C_2 R^2 l_s^3/(3R'^4 T_0 \sqrt{\alpha_s/\alpha_g})$. Figure 5 presents the calculated thermal expansion coefficient using $T_0 = 300\text{K}$ and $\alpha_g = 0.22\text{cm}^2/\text{s}$. The thermal expansion varied from $\sim 10 \times 10^{-6}$ to $\sim 100 \times 10^{-6}\text{K}^{-1}$ with the grain size, which is within the expected values for typical cements,[24] and presented similar behavior compared to the thermal diffusivity results as a function of gel volume.

The thermal diffusivity data can be compared with the porosity as a function of the gel volume and particle size of the cement powder. Figure 6 compares the distribution of particle sizes (a) in the CER25 samples with 140 and 160 μL gel volumes, and (b) in samples with 150 μL of CER25 and CER53. It is known that finer cement increases the rate of hydration and requires a large amount of liquid in the mixture to achieve set.[26,27] On the other hand, the porosity of the

TABLE I. OPC results for the thermal diffusivity of the samples.

Samples	Thermal diffusivity (10^{-3} cm^2/s)			
μL/650 mg	CER 25	CER 38	CER 45	CER 53
140	13 ± 1	8.8 ± 0.5	16 ± 3	48 ± 5
150	7 ± 3	8.0 ± 0.7	12 ± 3	45 ± 2
160	6.4 ± 0.3	7 ± 1	18 ± 3	41 ± 9
170	8.0 ± 0.8	12.1 ± 0.5	8.6 ± 0.6	60 ± 18
	MTA (this work)		Portland (this work)	
	46 ± 3		13.5 ± 0.5	
	Amalgam [24]	Ionomer [24]	Resin [24]	
	2.5 ± 0.1	4.8 ± 0.2	16.0 ± 0.6	

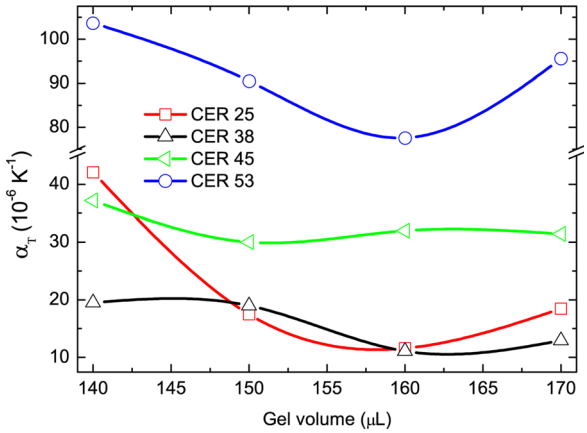

FIG. 5. (Color online) Thermal expansion of CER as a function of gel volume (uncertainty of 15%).

cement paste depends of the liquid-to-powder ratio.[26,28] Figure 5(a) shows an increase in the region of particle sizes from $(0.1-0.8)\mu$m to $(0.1-1.5)\mu$m when the gel volume was increased from 140 and 160 μL. The porosity also increased from 38.6% to 41.8%. The decrease observed in diffusivity could be due to the increase of gel retained into the pores. The gel is a polymer which generally has low thermal diffusivity values. The significant increase observed in thermal diffusivity when the particle size was increased from <25 to $<53\,\mu$m may have been caused by air trapped into the pores. The porosity is due to the incorporation of microscopic air bubbles during the mixing operation.[28] During hydration, the air bubbles are expelled from the material as the reaction products are going to fill up the pores. In coarser cement, the average interparticle pore spacing is larger, so that more hydration is needed to close off the capillary porosity.[27] For the CER53, the hydration products were not enough to fill completely the pores and, therefore, a greater amount of air was retained the cured material, increasing the thermal diffusivity. The presence of pores of larger diameter in CER53, Fig. 5(b), somewhat leads us to this conclusion.

Comparing both CER 25 and CER 38 groups, it can be noticed an increase in the intensity rate and width of the mercury absorption for CER 25 samples. In fact, this might

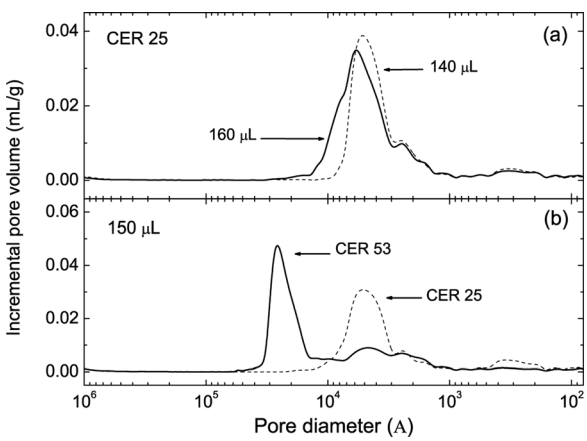

FIG. 6. Comparison of pore size distribution of the (a) CER 25 vs gel volume and (b) 150 μL gel volume vs CER powder particle size (CER 25 and CER 53).

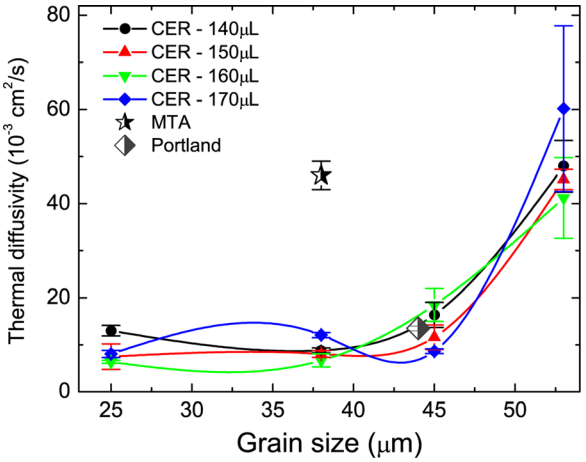

FIG. 7. (Color online) Thermal diffusivity of the samples as a function of grain sizes.

be related to an increase in the porosity allied to a larger pores distribution all over the bulk. For CER 38 prepared with 170 μL of gel, a larger distribution in pores sizes is observed. In other words, the porosity curves suggest that a high gel volume corresponds to a larger pore size distribution and porosity degree in the sample.

Figure 7 shows the thermal diffusivity as a function of the grain size for CER samples as well as the commercial MTA-Angelus and the Portland cements. It is possible to observe that thermal diffusivity presents a tendency to increase as the grain size increases. Up to 45 μm it varies slightly around 10×10^{-3}cm^2/s. On the other hand, grain size of 53 μm presented α_s as high as 60×10^{-3}cm^2/s, as shown for the CER53-170 μL. In fact, these high values occurred to all gel volume used in the samples preparation. It is worth noting the nearly constant value of the thermal diffusivity for a given grain size as a function of the gel volume. It could be due to a similar value of the thermal diffusivity of the particles and the gel.

The increase in the thermal diffusivity as the grain size increases can be explained based on the fact that the materials density remained approximately constant for different granulation and gel volumes. In this way, the larger the grain size, smaller is the effect of the heat-coupling between air and the solid material, and the thermal diffusivity increases. In other words, as the grain size decreases, the contact area between grain and air increases, and the thermal diffusivity diminishes.

The value of the thermal diffusivity of MTA-Angelus is similar to the one for the cement CER 53. The result for the Portland cement (prepared with grain size of 45 μm) is close

TABLE II. Typical materials sorted from [26] and tabulated for comparison to OPC data.

Commercial name	α_s (10^{-3} cm^2/s)	ρ (10^6 g/m^3)	c (J/gK)	k (10^{-2} W/cmK)
Marble	12 ± 2	2.7 ± 0.1	0.8 ± 0.2	2.6 ± 0.7
Achatit	2.9 ± 0.2	1.8 ± 0.4	1.3 ± 0.3	0.7 ± 0.2
Charisma	3.2 ± 0.2	2.0 ± 0.1	1.0 ± 0.2	0.7 ± 0.1
Dentinment	17 ± 2	13.3 ± 0.7	0.16 ± 0.03	3.6 ± 0.8

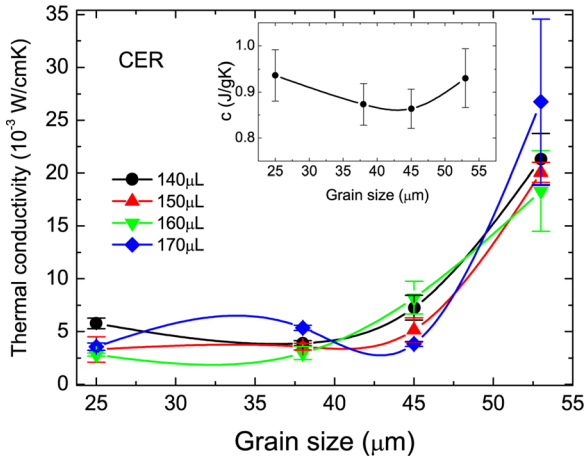

FIG. 8. (Color online) Thermal conductivity of the CER samples as a function of grain sizes.

to the one obtained for the cement CER considering the same granulation. This was expected since the cement CER is obtained from the Portland cement clinker.

Table II shows the thermal properties and mass density values obtained from the literature of some materials applied in dental restoration and components utilized in their production, as marble, for example. These results indicate that the thermal diffusivity values of the cement CER considering granulations until 45 μm are similar to those of Marble and Amalgamate (Dentinment). The case where the granulation 53 μm is considered, the values found are around $50 \times 10^{-3}\text{cm}^2/\text{s}$, being very close to the one determined for the MTA-Angelus. This result suggests that the granulation of 53 μm could have a significant increase of the porosity, and consequently in the thermal diffusivity.

The specific heat and mass density results for all CER samples were found to be very close to $(0.90 \pm 0.04)\text{J/gK}$ and $(2.5 \pm 0.3)\text{g/cm}^3$, respectively. Inset in Fig. 8 displays the grain size dependence of the specific heat for gel volume of 140 μL. The same behavior was also observed for gel volumes from 150 to 170 μL (not shown). Finally, knowing the values of the thermal diffusivity, heat specific and mass density, thermal conductivity can be calculated using $k = \rho c \alpha_s$. The results are shown in the Fig. 8 as a function of the grain size, showing the same behavior as displayed by the thermal diffusivity.

The obtained results using the OPC method on the CER samples reveal two important aspects. The first one was the correlation between the thermal transport properties (thermal diffusivity) with the porosity. The second one is the OPC technique providing the thermophysical parameters of the cement CER, which can help in the choice of an optimized formulation in terms of the needs of its application in dentistry.

VI. CONCLUSION

In this paper, we have demonstrated the applicability of OPC technique for evaluating the thermal properties of dental cements, providing information that can assist on the preparation process of the fast hardening cement. The measurement of thermal diffusivity was performed in samples with different gel/powder ratio and particle sizes and the results were compared to the ones from commercial cements. The results showed that the thermal diffusivity of CER tends to increase smoothly with gel volume and rapidly against particle size. This behavior was linked to the pores size and their distribution in the samples.

ACKNOWLEDGMENTS

The authors thank the Brazilian agencies CAPES, CNPq, FAPESP, and Fundação Araucária for their financial support.

[1]D. Almond and P. Patel, *Photothermal Science and Techniques* (Chapman and Hall, London, 1996).
[2]H. Vargas and L. C. M. Miranda, Phys. Reports **161**, 43 (1988).
[3]H. Vargas and L. C. M. Miranda, Rev. Sci. Instrum. **74**, 794 (2003).
[4]J. H. Rohling, J. Shen, J. Zhou, and C. E. Gu, Opt. Lett. **31**, 44 (2006).
[5]A. C. Boccara, D. Fournier, and J. Badoz, Appl. Phys. Lett. **36**, 130 (1980).
[6]A. Rosencwaig and A. Gersho, J. Appl. Phys. **47**, 64 (1976).
[7]O. Pessoa, C. L. Cesar, N. A. Patel, H. Vargas, C. C. Ghizoni, and L. C. M. Miranda, J. Appl. Phys. **59**, 1316 (1986).
[8]N. E. Souza, A. C. Nogueira, J. H. Rohling, M. L. Baesso, A. N. Medina, A. P. L. Siqueira, L. A. Sampaio, H. Vargas, and A. C. Bento, J. Appl. Phys. **106**, 093105 (2009).
[9]D. T. Dias, A. N. Medina, M. L. Baesso, and A. C. Bento, Appl. Spectrosc. **59**, 173 (2005).
[10]T. M. Coelho, E. C. Vidotti, M. C. Rollemberg, A. N. Medina, M. L. Baesso, N. Cella, and A. C. Bento, Talanta **81**, 202 (2010).
[11]A. C. Bento, H. Vargas, M. M. F. Aguiar, and L. C. M. Miranda, Phys. Chem. Glasses **28**, 127 (1987).
[12]N. G. C. Astrath, F. B. G. Astrath, J. Shen, C. Lei, C. J. Q. Zhou, Z. S. Liu, T. Navessin, M. L. Baesso, and A. C. Bento, J. Appl. Phys. **107**, 043514 (2010).
[13]T. M. Coelho, E. S. Nogueira, W. R. Weinand, W. M. Lima, A. Steimacher, A. N. Medina, M. L. Baesso, and A. C. Bento, J. Appl. Phys. **101**, 084701 (2007).
[14]W. M. Lima, W. R. Weinand, V. Biondo, E. S. Nogueira, A. N. Medina, M. L. Baesso, and A. C. Bento, Rev. Sci. Instrum. **74**, 716 (2003).
[15]S. J. Lee, M. Monsef, and M. Torabinejad, J. Endod. **19**, 541 (1993).
[16]M. Parirokh and M. Torabinejad, J. Endod. **36**, 16 (2010), Part I; M. Parirokh and M. Torabinejad, J. Endod. **36**, 190 (2010), Part II; M. Parirokh and M. Torabinejad, J. Endod. **36**, 400 (2010), Part III.
[17]J. E. Gomes-Filho, G. Rodrigues, S. Watanabe, P. F. Estrada Bernabé, C. S. Lodi, A. C. Gomes, M. D. Faria, A. Domingos dos Santos, and J. C. Silos Moraes, J. Endod. **35**, 1377 (2009).
[18]A. D. Santos, J. C. S. Moraes, E. B. Araujo, K. Yukimitu, and W. V. Valerio Filho, Int. Endod. J. **38**, 443 (2005).
[19]A. D. Santos, E. B. Araújo, K. Yukimitu, J. C. Barbosa, and J. C. S. Moraes, Oral Surgery, Oral Medicine, Oral Pathology, Oral Radiology, and Endodontology **106**, e77 (2008).
[20]M. D. da Silva, I. N. Bandeira, and L. C. M. Miranda, J. Phys. E. Sci. Instrum. **20**, 1476 (1987).
[21]A. N. Medina, A. M. F. Caldeira, A. C. Bento, M. L. Baesso, J. A. Sampaio, T. Catunda, and F. G. Gandra, J. Non-Cryst. Solids **304**, 299 (2002).
[22]P. Charpentier, F. Lepoutre, and L. J. Bertrand, J. Appl. Phys. **53**, 608 (1982).
[23]R. Holland, J. A. Otoboni, V. Souza, M. J. Nery, P. F. E. Bernabe, and E. Dezan, J. Endod. **27**, 281 (2001).
[24]J. O'Brien, *Biomaterials Properties Database* (Quintessence Publishing, Michigan, 1996).
[25]J. L. P. Molina, G. G. Juárez, R. H. Franco, I. V. Luna, P. Cholico, and J. J. A. Gil, Int. J. Thermophys. **26**, 243 (2005).
[26]A. M. Neville, *Properties of Concrete* (Pitman Books, London, 1973).
[27]D. P. Bentz, E. J. Garboczi, C. J. Haecker, and O. M. Jensen, Cement and Concrete Research **29**, 1663 (1999).
[28]M. Fridland, R. Rosado, and J. Endod. **29**, 814 (2003).